Clays and Clay Minerals, Vol. 41, No. 2, 162–177, 1993.

AN EXPERIMENTALLY DERIVED KINETIC MODEL FOR SMECTITE-TO-ILLITE CONVERSION AND ITS USE AS A GEOTHERMOMETER

WUU-LIANG HUANG, JOHN M. LONGO, AND DAVID R. PEVEAR

Exxon Production Research Company
P.O. Box 2189, Houston, Texas 77252-2189

Abstract—The smectite-to-illite conversion during shale diagenesis has recently been used to constrain the estimate of a basin's thermal history. We have systematically investigated the kinetics for the conversion of a Na-saturated montmorillonite (SWy-1) to a mixed-layer smectite/illite as a function of KCl concentration (from 0.1 to 3 moles/liter) over a temperature range of 250° to 325°C at 500 bars in cold-seal pressure vessels using gold capsules. The results show that the conversion rate can be described by a simple empirical rate equation:

$$-dS/dt = A \cdot \exp(-Ea/RT) \cdot [K^+] \cdot S^2$$

where S = fraction of smectite layers in the I/S, t = time in seconds, A = frequency factor = 8.08×10^{-4} sec^{-1}, exp = exponential function, Ea = activation Energy = 28 kcal/mole, R = gas constant, 1.987 cal/deg-mole, T = temperature (degree Kelvin), $[K^+]$ = K^+ concentration in molarity (M) in the fluid.

The results also show that Ca^{2+} in solutions barely affects the illitization rate, whereas Mg^{2+} significantly retards the rate. The retardation, however, is not as severe as previously reported. Na^+ ion can significantly retard the rate only if the concentration is high.

We found that by assuming a range 0.0026–0.0052 moles/liter (100–200 ppm) of K^+, concentrations similar to the value typically reported in oil field brines, the present kinetic model can reasonably predict the extent of the smectite-to-illite conversion for a number of basins from various depths and age. This narrow range of potassium concentrations, therefore, is used to model the smectite-to-illite conversion in shale when the actual chemical information of pore fluid is not available.

The kinetic equation has been tested using field data from a large variety of geologic settings worldwide (i.e., the Gulf of Mexico, Vienna Basin, Salton Trough Geothermal Area, East Taiwan Basin, Huasna Basin, etc). The results show that the equation reasonably predicts the extent of the reaction within our knowledge of the variables involved, such as burial history, thermal gradients, and potassium concentration.

Key Words—Geothermometry, Illite, Kinetics, Smectite, Smectite/illite.

INTRODUCTION

Smectite-to-illite conversion is the most important mineral reaction during shale diagenesis. Smectite commonly occurs in fine-grained sediments at shallow depths. During burial diagenesis, smectite is converted to illite, generally releasing silica, water, and cations in the process. This reaction has been suggested as a source of silica or carbonate cements for the host shale and adjacent sandstones, thereby significantly affecting the quality of a reservoir and its seal. Water released from this reaction may enhance hydrocarbon migration or form overpressure (e.g., Boles and Franks, 1979; Bruce, 1984). Most importantly, this reaction can serve as an independent geothermometer to constrain the proposed thermal history of a basin for better predicting source rock maturation (Pytte and Reynolds, 1989; Eslinger and Pevear, 1988; Elliot *et al.*, 1991).

The reaction also has received a great deal of academic interest because of the disputed nature of both mixed-layer illite/smectite (I/S) and the reaction mechanism (e.g., Reynolds and Hower, 1970; Garrels, 1984; Nadeau *et al.*, 1984; Środoń and Eberl, 1984; Bethke and Altaner, 1986; Sass *et al.*, 1987; Eberl *et al.*, 1990; Inoue *et al.*, 1987; Whitney and Northrop, 1988; Yau *et al.*, 1987). Many experiments have been carried out to convert smectite to illite or I/S hydrothermally. Most of these experiments were designed to focus on a variety of special problems such as conversion rates (Eberl and Hower, 1976), the effect of interlayer cations (Eberl, 1978), octahedral substitution (Güven and Huang, 1991), tetrahedral substitution (Huang and Otten, 1987), solution chemistry (Roberson and Lahann, 1981), kinetics of layer charge development (Howard and Roy, 1985), control of ordering of mixed-layers (Eberl, 1977; Inoue and Utada, 1983; Bethke *et al.*, 1986; Huang, 1989), conversion mechanism (Whitney and Northrop, 1988), and the effect of flow rate in flow through experiments (Kacandes *et al.*, 1991).

There are few published reports on the kinetics of this important reaction. Eberl and Hower (1976) concluded that the illitization rate of synthetic beidellites follows first-order kinetics. However, this kinetic model is not applicable to field observations because the

illitization rate of the synthetic smectite is found to be significantly lower than that of natural smectite (Eberl and Hower, 1976; Huang and Otten, 1987). Bethke and Altaner (1986) derived a theoretical rate law by assuming the layer-by-layer substitution mechanism of smectite to illite transformation. Pytte and Reynolds (1989) derived a sixth-order kinetic equation based on the field observations of progressive illitization of smectite in a contact metamorphic zone. The sixth-order kinetic equation has been widely used for modeling smectite-to-illite conversion in nature (e.g., Altaner, 1989; Elliot *et al.*, 1991). Recently, an empirical kinetic model was proposed by Velde and Vasseur (1992) based on field data from three sedimentary basins.

The present study aims to quantify the kinetics of the smectite-to-illite reaction experimentally using natural smectite in order to forecast accurately the timing of the conversion. We focus on the effect of important parameters such as temperature and potassium concentration on the conversion rate. These results enabled us to develop a new kinetic equation for modeling the smectite-to-illite reaction during shale diagenesis.

EXPERIMENTAL MATERIALS AND PROCEDURES

Starting smectite

The starting smectite used for smectite-to-illite conversion experiments is montmorillonite (SWy-1) from Crook County, Wyoming, and was supplied by the Source Clay Mineral Repository, Department of Geology, University of Missouri. Four different batches of starting smectite were prepared using different procedures (Table 1).

Batch #1 represents a purified sample that was prepared using the following procedure: The <2 μm size fraction was obtained by suspension and centrifugation of SWy-1 clay; this fraction was then placed in a saturated NaCl solution; the Na-saturated sample was then mixed with sodium acetate solution (pH 5) and heated to 85°C to remove carbonates; organic impurities in the sample were removed with H_2O_2 at <80°C, then the sample was washed with distilled water. Iron oxides were removed with a solution of Na-citrate, Na-bicarbonate, and Na-dithionite; the sample was then washed again with distilled water. Finally, the salt in solution was removed by dialysis, and the purified sample was freeze-dried. Batches #2 and #3 were prepared using the <2 μm fraction of Na-saturated SWy-1 clay, then freeze-dried. Carbonate, organics, and iron oxide removal were not performed for these two samples. Batch #4 was prepared using the <2 μm fraction of Na-saturated SWy-1 clay, then air-dried. Impurity removal was not performed.

Initial experiments used a purified and freeze-dried sample (Batch #1). Later we found the conversion rate of the purified and freeze-dried sample (Batch #1) significantly different from that of the unpurified samples. In order to better simulate natural shale diagenesis, the unpurified and air-dried sample (Batch #4) was used in most runs. The use of different batches of the starting sample in the experiments partially accounts for the scatter of the data.

Experimental procedures

Mixtures of starting Na-saturated montmorillonite (SWy-1) with quartz powder were reacted in solutions with a KCl concentration ranging from 0.1 M to 6 M and fluid/rock ratio from 5 to 10 in cold-seal pressure vessels at temperatures from 250°C to 325°C and 500 bars. Additional experiments with solutions containing Na^+, Mg^{2+}, and Ca^{2+} ions were also performed in order to simulate reaction during shale diagenesis. Gold capsules were used as sample containers for all experiments. The solid run products were washed with distilled water on filter paper to remove excess KCl from the samples. These samples were ultrasonically dispersed using 10 mg of sample in 0.5 ml of distilled water. They were then sedimented onto a glass slide, with sample coverage within an area 19 mm $\times$ 19 mm. Samples were solvated by placing the oriented mount in a desiccator over ethylene glycol at room temperature overnight. The solvated samples were examined by X-ray diffraction (XRD) for the illite/smectite ratio of mixed-layer clays using the NEWMOD (R. C. Reynolds, IBM PC-AT Version 1.0, 1985; Reynolds, 1980) computer program. The uncertainty of measurement of percent of illite in the I/S sample is considered to be $\pm 5\%$; however, the overall uncertainty for % I is estimated to be $\pm 15\%$ when taking the uncertainty of the experimental temperature and the variation of the starting smectite sample into account. Selected run products were also resaturated with Na^+ in 1 M NaCl solution (S. P. Altaner, personal communication, 1992). The results show that the expandability of the neoformed I/S significantly increases after being resaturated with Na, results similar to those found by Whitney and Northrop (1988). The observation probably indicates that part of the neoformed 2:1 layer has created interlayer charge only marginally for K fixation, probably due to the high temperature/short time used in the experiments in contrast to the low temperature/long time for natural samples that hardly show such behavior. While the mechanism behind this behavior requires further study, this paper, as well as Whitney and Northrop's (1988), used the expandability measured from the untreated run products to calculate the % I (or S) layers in the neoformed I/S.

The pH of solutions from experiments were measured, but there was insufficient solution for elemental analysis. However, the final K^+ concentration $[K^+]$ in the solution can be calculated from the extent of the reaction. In fitting our experimental data to the kinetic

Table 1. Experimental results for kinetics of smectite/illite conversion.

Run no.	Time (days)	Starting materials: Solid: Smectite batch	Starting materials: Solution: KCl (M)	Fluid/rock μl/mg	Run products: % Illite in S/I	Run products: Stacking order $P_{S\text{-}I}$[1]	Run products: Discrete illite	Run solutions: Quench pH	Run solutions: Average[2] $[K^+]$ (M)
				325°C					
CS496	0.625	No. 4	1	10	23	R0	No	3.47	0.98
CS487	1	No. 4	1	10	42	0.46	Tr.	3.61	0.97
CS488	3	No. 4	1	10	67	R1	Tr.	3.52	0.97
CS506	1	No. 4	0.6	10	50	0.55	No	3.86	0.55
CS497	3	No. 4	0.6	10	65	R1	No	3.41	0.57
CS498	6	No. 4	0.6	10	70	R1	No	3.44	0.57
CS499	6	No. 4	0.3	10	60	0.75	No	3.76	0.27
CS500	12	No. 4	0.3	10	60	R1	No	3.97	0.27
CS490	12	No. 4	0.1	10	25	R0	No	4.80	0.082
CS493	34	No. 4	0.1	10	37	0.39	No	4.66	0.077
				300°C					
CS429	1	No. 1	6	5	40	0.41	Yes	3.45	5.95
CS459	1.67	No. 3	6	5	50	0.51	Yes	3.63	5.94
CS461	2.3	No. 3	6	5	55	0.70	Yes	3.96	5.94
CS457	3	No. 3	6	5	65	0.90	Yes	3.17	5.94
CS402	2	No. 1	3	5	50	0.54	No	3.33	2.95
CS455	2.6	No. 3	3	5	48	0.52	Tr.	3.53	2.95
CS456	3	No. 3	3	5	55	0.60	Tr.	3.49	2.94
CS458	3.6	No. 3	3	5	58	0.74	Tr.	3.63	2.94
CS448	3.6	No. 1	3	5	63	0.95	Tr.	3.51	2.94
CS395	5	No. 1	3	5	66	R1	No	3.47	2.94
CS403	2	No. 1	1	5	32	R0	No	3.43	0.95
CS396	5	No. 1	1	5	45	0.56	Tr.	3.50	0.95
CS451	7	No. 2	1	5	63	R1	Tr.	3.45	0.94
CS510	5	No. 4	0.6	10	55	R0	No	4.20	0.55
CS400	5	No. 1	0.3	5	25	R0	Tr.	3.49	0.26
CS449	22	No. 1	0.3	5	35	R0	No	3.84	0.25
CS460	27	No. 3	0.3	5	42	0.52	No	4.13	0.25
CS437	30	No. 1	0.3	10	53	0.75	No	3.86	0.27
CS397	5	No. 1	0.1	5	16	R0	No	4.20	0.074
CS513	61	No. 4	0.1	10	37	0.47	No	4.17	0.08
				275°C					
CS478	3	No. 4	3	10	20	R0	No	3.76	2.98
CS474	5	No. 4	3	10	43	0.49	No	3.46	2.98
CS503	8	No. 4	3	10	57	0.59	No	3.86	2.97
CS501	2	No. 4	1	10	15	R0	No	4.28	0.99
CS479	5	No. 4	1	10	37	R0	No	3.73	0.98
CS475	10	No. 4	1	10	50	0.55	No	3.65	0.97
CS502	15	No. 4	0.5	10	35	R0	No	4.56	0.47
CS494	21	No. 4	0.1	10	20	R0	No	5.69	0.085
CS495	45	No. 4	0.1	10	20	R0	No	4.97	0.085
				250°C					
CS508	8	No. 4	3	10	20	R0	No	4.54	2.98
CS509	15	No. 4	3	10	35	R0	No	4.09	2.97
CS486	80	No. 4	3	10	75	R1	No	3.59	2.97
CS485	40	No. 4	1	10	35	0.39	No	3.96	0.98
CS511	60	No. 4	1	10	55	0.58	No	4.14	0.97

[1] For $P_I < 0.5$, $P_{S\text{-}I} = (P_I \cdot P_{I\text{-}S})/P_S$, where $P_{I\text{-}S}$ equals $P_{B\text{-}A}$, which can be obtained from NEWMOD modeling. For $P_I > 0.5$, $P_{S\text{-}I}$ equals $P_{B\text{-}A}$.

[2] Average of starting and final $[K^+]$ in experimental solution; see text for calculating final $[K^+]$ in solution.

model, we assume $[K^+]$ to be constant during the experiment. The $[K^+]$ obtained by averaging initial and final $[K^+]$ was used for this calculation. The uncertainty caused by this assumption is small and acceptable for those runs with high $[K^+]$ (>0.1 M) but can be significant for runs with lower $[K^+]$ and high percentage of conversion. For runs with low $[K^+]$, a high fluid/rock ratio was used to reduce the change in $[K^+]$ during experiments. The calculated average K concentration and run conditions used for the kinetic study are listed

https://doi.org/10.1346/CCMN.1993.0410205 Published online by Cambridge University Press

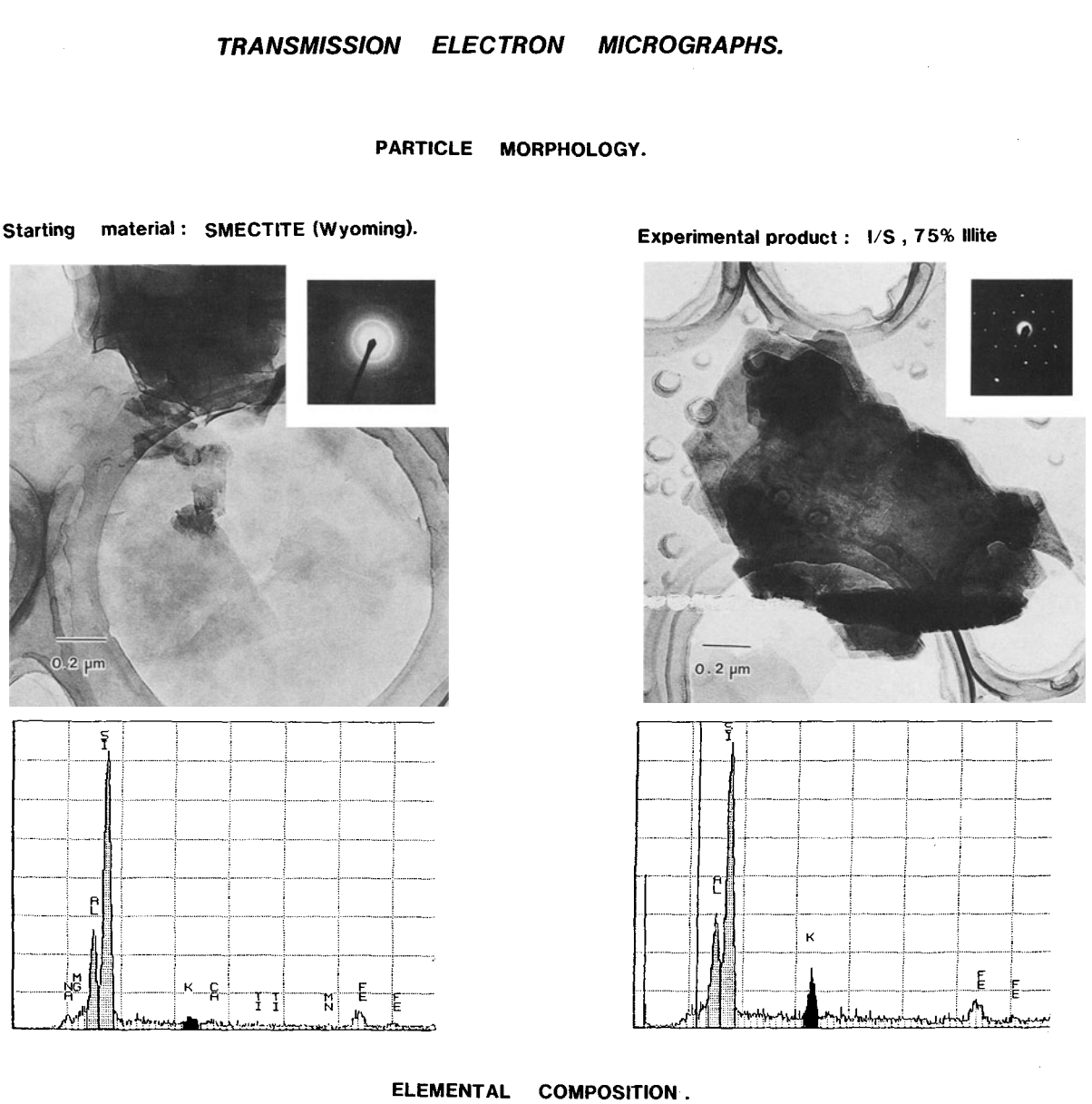

Figure 1. TEM micrographs of starting smectite and smectite/illite formed in the experimental run products.

in Table 1. The detailed experimental procedures are similar to those previously reported (e.g., Huang, 1992).

EXPERIMENTAL RESULTS

Our experiments were designed firstly to quantify the effect of potassium concentration and temperature on the kinetics of the smectite-to-illite reaction and secondly to determine the effect of cations such as Na^+, Ca^{2+}, and Mg^{2+} on the conversion rate. Only the experimental data and discussion relevant to the development of the kinetic model are reported in this paper. Detailed experimental studies including the nature of the neoformed I/S, smectite/illite equilibrium, control of I/S ordering and the reaction mechanism will be published elsewhere.

Rates of smectite-to-illite conversion

We have systematically investigated the kinetics for the conversion of a Na-montmorillonite to mixed-layer illite/smectite (I/S) as a function of [KCl] concentration (0.1 to 6 M) over a temperature range of 250° to 325°C. Figure 1 shows transmission electron micrographs (TEM) and elemental spectrum of a starting smectite (S) and of an I/S with 75% illite layers (%I) produced in experiments. The TEM study shows a significant change in morphology as well as chemistry of the clay particles as a result of conversion. Note the

https://doi.org/10.1346/CCMN.1993.0410205 Published online by Cambridge University Press

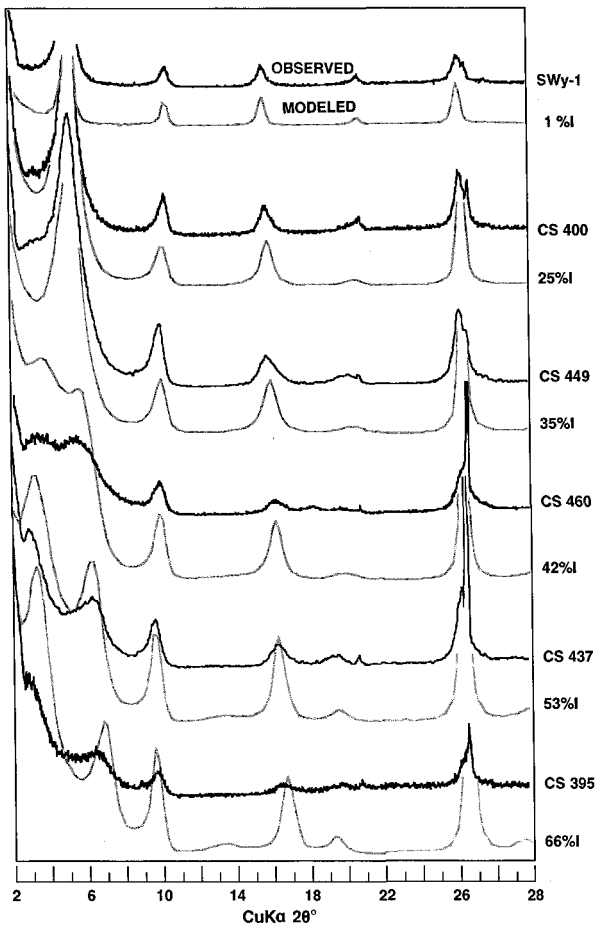

Figure 2. Examples of XRD patterns for starting smectite and I/S experimentally converted from smectite. The calculated patterns using the program NEWMOD are also shown for comparison.

rigid and platelet-like I/S with significant amounts of potassium in contrast to flaky smectite containing no potassium (Figure 1). I/S with high expandability in run products exhibits curled flakelike habit, whereas I/S with low expandability has a lath or equant platelet appearance. The morphological change during conversion is similar to that observed in the synthetic systems (Güven and Huang, 1991) as well as in natural hydrothermal environments (Inoue *et al.*, 1987). Detailed morphology and particle size change as a function of reaction extent is currently under investigation (R. E. Klimentidis, personal communication). TEM also shows the presence of amorphous silica and quartz in the run products. The distinction between the amorphous silica, neoformed quartz, and the quartz initially present in the starting solid is mainly based on the morphology.

The pH of quench solutions in most runs is significantly lower than that of the initial solution. The significant decrease in pH appears to occur at a very early stage of the reaction, perhaps before the smectite-to-illite conversion. The results show no systematic variation of quench pH as a function of the extent of smectite-to-illite conversion observed by XRD (Table 1).

The percentage of illite layers and degree of ordering of the neoformed clay were determined by matching the experimental XRD pattern with the calculated pattern (Figure 2). Trace amounts (<3%) of discrete illite in addition to I/S were identified in some run products, particularly in runs using high [K^+] solutions (Table 1) and were ignored in calculating the illitization rate. Our experimental results (% illite in I/S *vs* time for each [K^+]) at 325°, 300°, 275°, and 250°C are shown in Figure 3A–D and listed in Table 1. These data are fitted to a kinetic equation that enables us to extrapolate the high temperature and high K concentration data to diagenetic conditions.

Effects of other cations on kinetics

We have also investigated the effect of other cations such as Na^+, Mg^{2+}, and Ca^{2+} on the kinetics of the smectite-to-illite conversion in the presence of 0.6 M K^+ at 300°C. The results show that the conversion rate can be retarded in the presence of significant amounts of Mg^{2+} and Na^+ ions. Our results show that, at 300°C for 3 days, smectite converts to I/S with 45% illite in a 0.6 M KCl solution but yields only 30% illite in the same solution containing 4950 mg/liter Mg^{2+} (0.2 M). However, in order to retard illite formation as much as Mg-bearing solutions do, a solution with 135,000 mg/liter Na^+ (5.9 M) is required. This suggests that Mg ions more effectively retard the smectite-to-illite conversion than Na^+. Our results also show that the effect of these cations is more severe at early stages of conversion (for instance, 3 days *vs* 10 days in our experiments, Table 2). As the conversion approaches 60% illite in I/S, the effects of Mg^{2+} and Na^+ become insignificant. The experimental results for the effect of different cations are listed in Table 2.

In general, our results show that the conversion rate is only slightly affected by [Na^+] and [Mg^{2+}] unless concentrations are very high ([Na^+] >50,000 ppm, [Mg^{2+}] >1500 ppm) relative to average oil field brine ([Na^+] = 9400 ppm, [Mg^{2+}] = 127 ppm). The results also show that Ca^{2+} ions, in contrast to Mg^{2+} and Na^+, barely affect the smectite-to-illite conversion rate. The results are significantly different from those obtained by Roberson and Lahann (1981) using Cambers or Polkville montmorillonite in solution with a fluid/rock ratio (110:1) that is much higher than that (5:1) of this study. In the study of Na^+ effect, both studies used Na-saturated montmorillonite in KCl + NaCl solutions and showed the retardation of the rate is comparable in terms of [Na^+]/[K^+] ratios. In the study of Mg^{2+} effect, both studies used Na-saturated montmorillonite

https://doi.org/10.1346/CCMN.1993.0410205 Published online by Cambridge University Press

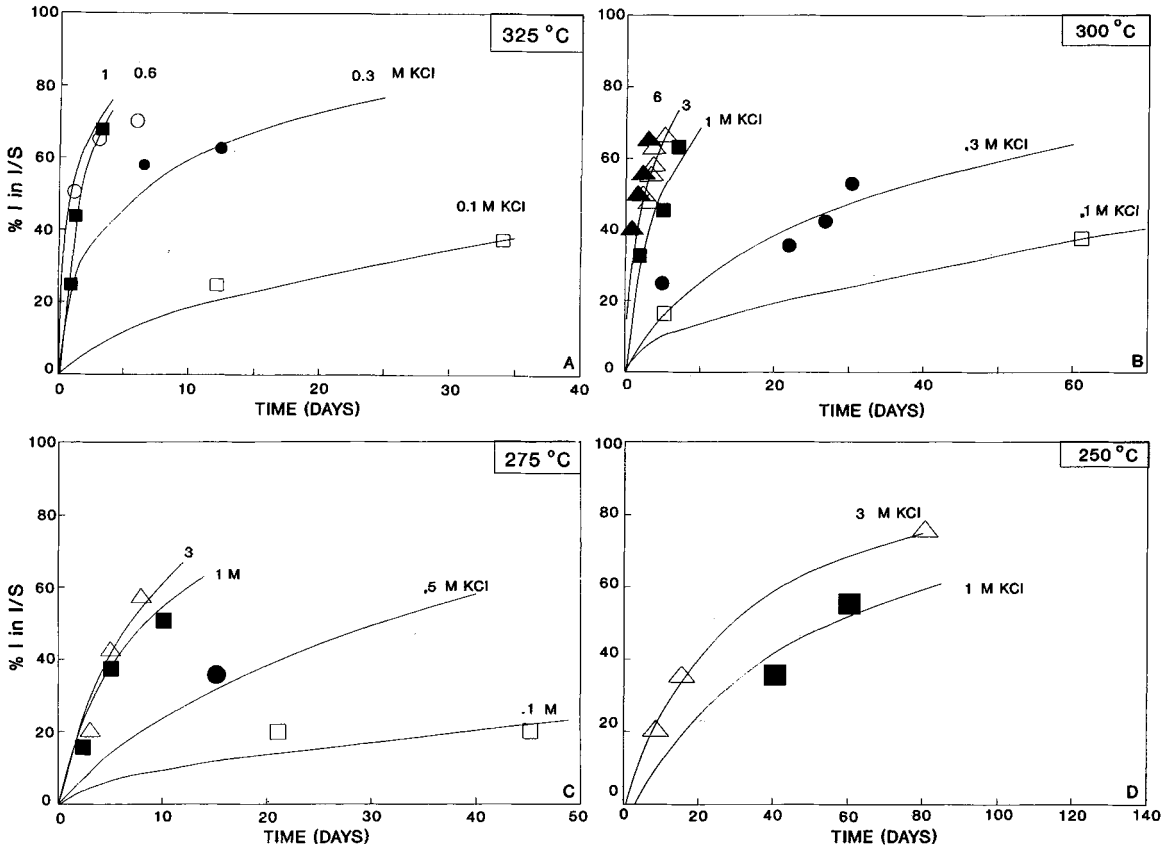

Figure 3. Experimental results showing the increase of % of illite in mixed-layer I/S as a function of $[K^+]$ and time at different temperatures: A) 325°C, B) 300°C, C) 275°C, and D) 250°C.

Table 2. Experimental data for studying the effect of cations on smectite/illite conversion.

Run no.	Time (days)	KCl (M)	Other salt Type	Other salt Conc. (mg/l)	% Illite in I/S	Stacking order (P_{s-1})	Quench pH
CS560	3	0.6	—	—	45	0.53	3.84
CS556	10	0.6	—	—	60	R1	—
CS535	30	0.6	—	—	68	R1	3.96
CS539	63	0.6	—	—	68	R1	3.98
CS561	3	0.6	NaCl	135,000	30	R0	3.72
CS554	10	0.6	NaCl	135,000	52	0.78	3.98
CS532	30	0.6	NaCl	135,000	66	R1	3.45
CS540	63	0.6	NaCl	135,000	68	R1	3.81
CS531	30	0.6	NaCl	27,000	66	R1	3.73
CS530	30	0.6	NaCl	2,700	66	R1	3.85
CS564	3	0.6	$MgCl_2$	57,160	20	R0	4.08
CS563	3	0.6	$MgCl_2$	4,950	30	R0	3.61
CS555	10	0.6	$MgCl_2$	4,950	50	0.6	3.92
CS533	30	0.6	$MgCl_2$	4,950	66	R1	3.47
CS541	63	0.6	$MgCl_2$	4,950	66	R1	3.51
CS562	3	0.6	$CaCl_2$	1,108	45	?	4.04
CS551	10	0.6	$CaCl_2$	1,108	60	R1	5.39
CS537	63	0.6	$CaCl_2$	1,108	72	R1	3.65
CS552	10	0.6	$CaCl_2$	490	60	R1	4.45
CS570	3	0.6	NaCl $+MgCl_2$	135,000 4,950	30	R0	5.05

https://doi.org/10.1346/CCMN.1993.0410205 Published online by Cambridge University Press

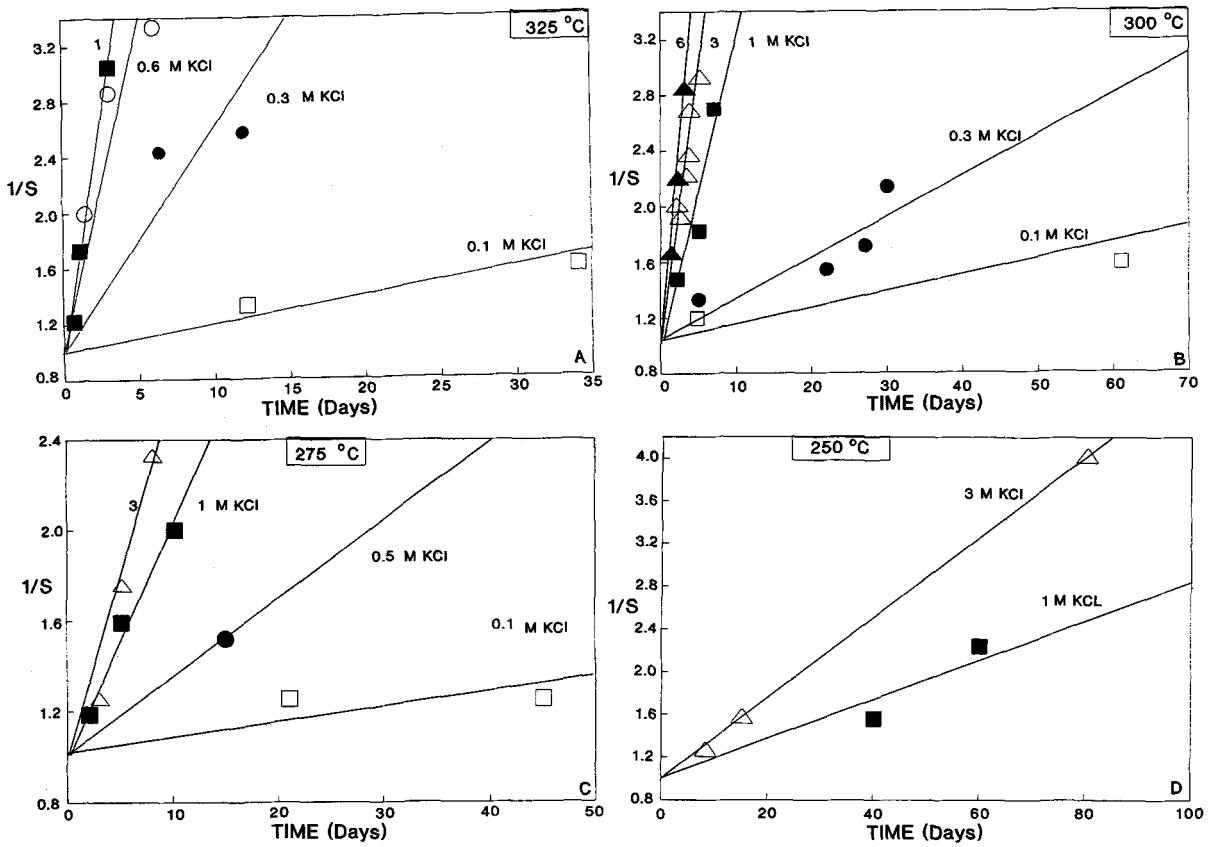

Figure 4. Experimental data fit to second order kinetic model at A) 325°C, B) 300°C, C) 275°C, and D) 250°C. The slopes of lines are the rate coefficient k′ for each $[K^+]$ and temperature.

in KCl and $MgCl_2$ solutions and found a significant retardation of the reaction rate. However, the effect of $[Mg^{2+}]$ on the rate is much more severe in Roberson and Lahann's (1981) experiments than in ours. The discrepancy is tentatively attributed to the higher $[Mg^{2+}]/[K^+]$ ratios used in their study than in ours. Further study on the effect of Mg^{2+} ion in solutions with low $[K^+]$ or high $[Mg^{2+}]/[K^+]$ ratios may resolve this discrepancy. In the study of the Ca^{2+} effect, they compared the rate for Na and Ca-saturated montmorillonite in KCl solution and found a significantly different rate, whereas we compared Na-saturated montmorillonite in KCl and KCl + $CaCl_2$ solutions and found no significant difference in rate. The pre-occupancy of Ca^{2+} in the interlayer space of smectite in their experiments may account for the significant retardation of illitization rate, which did not occur in our experiments using Ca-bearing solution. Further investigation on the mechanism that influences the illitization is ongoing to resolve the discrepancy. Based on the preliminary results of the present study, we tentatively apply our kinetic data to model the conversion rate during shale diagenesis without considering the effect of cations other than K^+. However, for hypersaline conditions, we have derived simple equations based on our limited experimental data to incorporate the effect of these cations on the kinetic model.

KINETIC MODEL OF SMECTITE-TO-ILLITE CONVERSION

Development of kinetic model

The experimental data (Table 1) for a given temperature and $[K^+]$ are plotted in terms of 1/S *vs* time (t), where S is the fraction of smectite in I/S in run products. Figure 4A–D show kinetic diagrams constructed from our experimental data for solutions with $[K^+]$ concentrations ranging from 0.1 to 6 M, respectively, at 325°, 300°, 275°, and 250°C. The results show that a linear relationship between 1/S *vs* t can be established within the uncertainty of experiments. The linear relationship of the plots (Figure 4) suggests that the conversion rate can be described by a kinetic model that is second-order with respect to the smectite fraction in the I/S (see Appendix A for detailed derivation). The empirical kinetic model can be expressed as:

$$-dS/dt = k'S^2 \quad (1)$$

where t is time and k′ is the rate coefficient for a given $[K^+]$.

https://doi.org/10.1346/CCMN.1993.0410205 Published online by Cambridge University Press

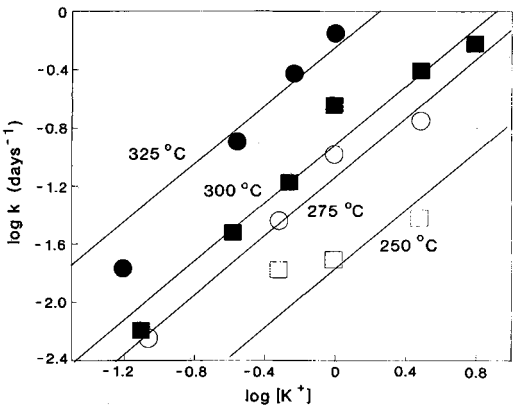

Figure 5. Experimental results showing the linear relationship of the logarithm of rate constant and potassium concentration at 325°C, 300°C, 275°C and 250°C.

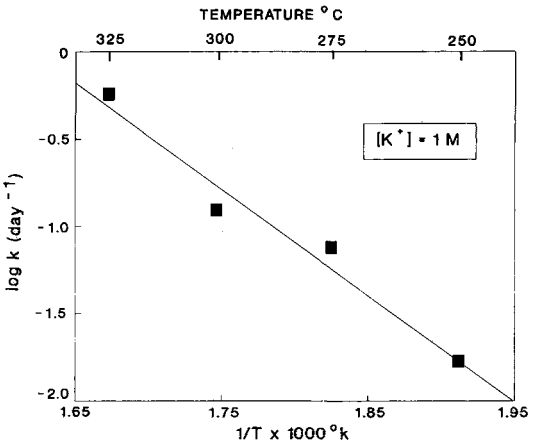

Figure 6. Experimental results are consistent with Arrhenius equation. The rate constant (k) was average k value for each temperature at $[K^+] = 1$ M (see Figure 5).

In addition, our results show that the smectite-to-illite conversion rate increases with increasing $[K^+]$ of the reaction solutions. The effect of $[K^+]$ on the conversion rate (log k′ *vs* log$[K^+]$) follows a linear relationship with a slope close to one for data at 300°C (Figure 5). The slope ($\simeq 1$) of the linear relationship suggests that the conversion rate can be described by a kinetic model which is first-order with respect to $[K^+]$ (Appendix A). Thus the rate equation becomes:

$$-dS/dt = k \cdot [K^+] \cdot S^2 \qquad (2)$$

where k is the rate constant which is a function of temperature. From Eqs. 1 and 2 we have $k' = k \cdot [K^+]$.

Data obtained at other temperatures (250°, 275° and 325°C) also confirm this kinetic relationship (Figure 5), which additionally defines the effect of temperature on the conversion rate. Figure 6 is an Arrhenius plot showing the relationship between rate constant (k) and temperature (log k *vs* 1/T). Our experimental data are consistent with this Arrhenius relationship:

$$k = A \cdot \exp(-Ea/RT) \qquad (3)$$

When fit to the relationship, our data give Ea = 28 Kcal/mole and $A = 8.08 \times 10^4$ $sec^{-1}mole^{-1}$ liter for all studied $[K^+]$, where A is the frequency factor, Ea is the activation energy, R is the gas constant, T is temperature °K, and exp is the exponential function. The overall kinetics of the smectite-to-illite conversion thus can be described by the equation:

$$-dS/dt = A \cdot [K^+] \cdot S^2 \cdot \exp(-Ea/RT) \qquad (4)$$

Under the hypersaline conditions, we use a cation factor C_n instead of $[K^+]$ in the kinetic Eq. 4, where

$$C_1 = [K^+] - (([K^+]/2) \cdot ([Na^+]/2.3))$$

for Na-rich subsurface fluid. (5)

$$C_2 = [K^+] - (([K^+]/2) \cdot ([Mg^{2+}]/0.05))$$

for Mg-rich subsurface fluid. (6)

$$C_3 = (C_1 + C_2)/2$$

for both Na- and Mg-rich fluid. (7)

These equations provide a more accurate prediction of smectite-to-illite conversion at hypersaline conditions if the brine chemistry data of the studied formation are available.

Discussion

The observed kinetic relationship, although empirical, is consistent with the principles of chemical kinetics (Lasaga, 1981), which suggest that the rate constant is, in general, proportional to the activity products of the reactants. Accordingly, our kinetic model, which is second-order with respect to smectite and first-order with respect to K^+ concentration, predicts that the smectite-to-illite conversion occurs following a reaction in which two smectite "molecules" react with one K^+ ion to form one "molecule" of illite. The proposed mechanism is supported by the stoichiometric relationship of the reaction (Eq. 8).

The chemical equation for this conversion can be written by assuming that Al is conserved in this reaction [similar to Reaction 2 in Boles and Franks (1979)]:

$$2\,\underset{\text{(Smectite)}}{Na_{0.4}(Al_{1.47}Mg_{0.29}Fe_{0.18})Si_4O_{10}(OH)_2} + 0.85\,K^+ + 1.07\,H^+$$

$$\rightarrow 1.065\,\underset{\text{(Illite)}}{K_{0.80}(Al_{1.98}Mg_{0.02})(Si_{3.22}Al_{0.78})O_{10}(OH)_2}$$

$$+ 4.6\,SiO_2 + 0.36\,Fe(OH)_3 + 0.56\,Mg^{2+}$$

$$+ 0.8\,Na^+ + 0.9\,H_2O \qquad (8)$$

The formula of the starting smectite in this equation is calculated from the chemical analysis reported in Van Olphen and Fripiat (1979) for the SWy-1 montmorillonite by assuming that all calcium was exchanged by Na during the Na-saturation. The neo-

https://doi.org/10.1346/CCMN.1993.0410205 Published online by Cambridge University Press

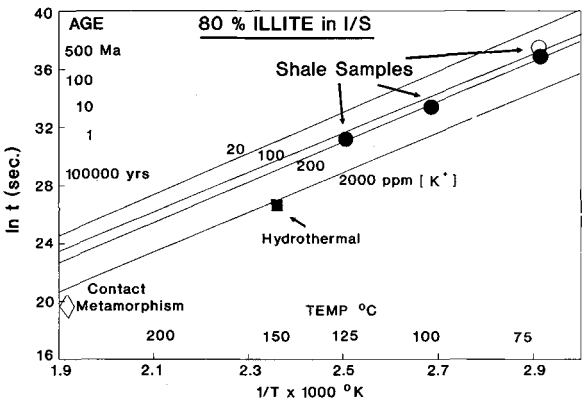

Figure 7. Time/temperature/[K^+] relationships calculated from the kinetic model for the conversion of smectite to mixed-layer illite/smectite with 80% illite layers. The kinetic model using [K^+] in a range similar to that in average oil field brine (100–200 ppm) reasonably predicts the extent of illitization for four carefully studied shales (Pytte and Reynolds, 1989) from various depths and ages (symbols: ○ = K-bentonite (450 Ma), ● = shale (300 Ma), shale (10 Ma) and shale (1 Ma)). Additional field data for samples from a hydrothermal well (Jennings and Thompson, 1986) and contact metamorphic rock (Reynolds, 1981, cited in Pytte and Reynolds, 1989) are also shown. Significantly higher [K^+] concentrations are required to model the observed 80% of smectite-to-illite conversion for these samples than those for shales and bentonite.

formed illite formula is calculated from Eq. 8 by assuming Al conservation and assuming a similar amount of Al substitution for Si in tetrahedral site as that in a natural illite composition [e.g., Grundy illite ($K_{0.56}$ $Na_{0.04}$ ($Al_{1.9}Mg_{0.24}$) ($Si_{3.22}Al_{0.78}$)$O_{10}(OH)_2$): Reesman, 1978]. Because of the lack of composition of neoformed illite, there is a large uncertainty for the above reaction formula. The kinetic mechanism which is second-order with respect to the fraction of smectite may alternatively indicate that the surface area of smectite controls the reaction kinetics.

FIELD TESTING OF THE SMECTITE/ILLITE KINETIC MODEL

K^+ concentration in shale fluids

Our experimental results suggest that variation of [K^+] in shale pore fluids can affect the smectite-to-illite conversion rate by as much as an order of magnitude. Therefore, in order to model accurately the conversion kinetics, information about the [K^+] of pore fluids in the studied formation is required. Because of the general lack of analytical data for shale fluid, the present study attempts to estimate indirectly the [K^+] in shale fluids using our kinetic model and the observed extent of smectite-to-illite conversion for four studied shales cited in Pytte and Reynolds (1989).

By integration of the kinetic Eq. 4 using boundary conditions, $S_o = 1$ at $t_o = 0$ at constant T, we have

$$S = S_o/(1+S_o\cdot[K^+]\cdot A\cdot\exp(-Ea/RT)\cdot t) \quad (9)$$

where S_o is the smectite fraction in the initial I/S. Using this equation, we are able to calculate a relationship among temperature, time period, and [K^+] for 80% smectite-to-illite conversion. The results for 20, 100, 200, 2000 ppm of [K^+] are plotted on Figure 7.

Data for six mixed-layer smectite/illite samples reported by Pytte and Reynolds (1989) are also plotted on the same diagram in Figure 7. Four samples are diagenetic, one is a contact metamorphic bentonite, and another is hydrothermal. All of these samples contain 80% illite. The results show that the calculated [K^+] for four shales (one is bentonite) of diagenetic origin all fall within the range 100 to 200 ppm. This finding suggests that, in the absence of chemical analysis of shale fluid, modeling shale diagenesis may be reasonably done by assuming a [K^+] of 200 ppm in the shale fluids, which is close to the average [K^+] in subsurface oil field brines (125 ppm) mainly from sandstone reservoir or sea water (380 ppm) (Broecker and Oversby, 1971). Using this potassium concentration, we are able to predict reasonably the extent of the smectite conversion to illite when the actual chemical information of pore fluid in shale is not available (see case studies in next section).

Two samples in Figure 7 are from contact metamorphic (Reynolds, 1981) and hydrothermal zones (Jennings and Thompson, 1986) and fall in a range of higher [K^+]. This indicates that the [K^+] in hydrothermal and contact metamorphic fluid is significantly higher than in shale and bentonite. This is consistent with observations that show the increase of K/Na ratio in geothermal fluids with increasing aquifer temperatures (e.g., Kharaka and Mariner, 1989).

The mechanism that controls the [K^+] in shale within this narrow range is not fully understood. We have calculated the [K^+] in solutions by equilibrating sea water with illite (with/without K-feldspar) using the geochemical modeling program Gt (C. M. Bethke, University of Illinois). Anhydrite was suppressed during the calculation. The calculation was done for near-neutral solution (pH of pure water at 80°C is 6.35 or log $Kw_{80°C}$ = 12.61) at pH 6.1 and 6.5 (fixed during calculation), each pH calculated at both 60° and 100°C. Although the pH of shale water is rarely reported, the assumption of near-neutral pore water in shale is reasonable for most shales due to their buffering capability. Our Gt modeling confirms that the initial pH 8.2 of seawater in contact with illite drifts to 5.5 at 100°C; the final equilibrium mineral assemblage includes quartz, muscovite, kaolinite, and smectite. The mineral assemblages saturated with the equilibrium solutions can be categorized into two major groups: one containing illite (or muscovite), kaolinite, and quartz with or without saponite and showing a lower [K^+] in

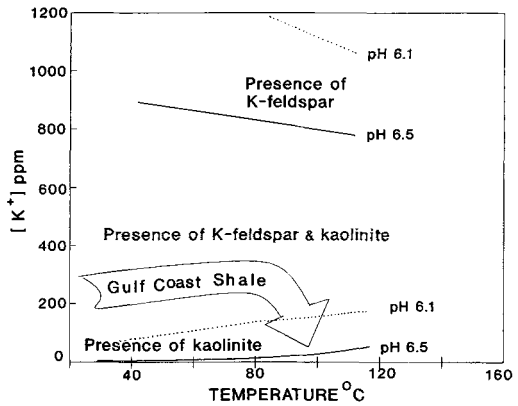

Figure 8. Potassium concentration of pore fluid (seawater composition) in equilibrium with K-feldspar + illite + quartz with or without phengite or illite + kaolinite + quartz with or without saponite as a function of temperature calculated for two fixed pH using the program Gt. The arrow indicates the possible evolution path of $[K^+]$ in the pore fluid of shale containing both kaolinite and K-feldspar such as found in the U.S. Gulf coast. $[K^+]$ tends to approach to the illite + kaolinite + quartz boundary as K-feldspar is consumed.

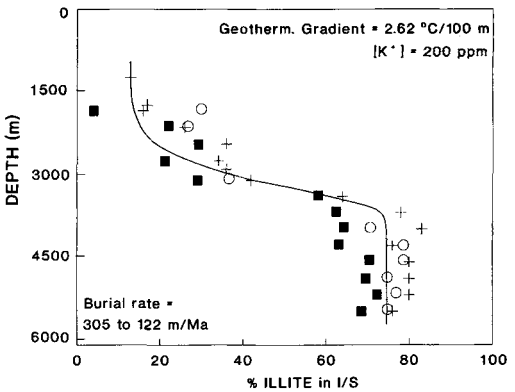

Figure 9. Comparison of modeled and observed smectite/illite conversion found in CWRU Gulf Coast well 6 shale (Hower *et al.*, 1976). Kinetic model predicts the smectite-to-illite conversion by reasonably estimating the geological parameters, such as potassium concentration ($[K^+]$), temperature and age at each depth, for the studied area. Line indicates modeling result whereas symbols indicate field data: cross = <0.1 μm, circle = 0.1 to 0.5 μm and square = 0.5 to 2 μm.

the solution (e.g., 30 ppm at pH 6.5, 80°C); and a second group containing illite (muscovite), K-feldspar (microcline), and quartz with or without phengite and showing a higher $[K^+]$ in the solution (e.g., 800 ppm at pH 6.5, 80°C, see Figure 8). The equilibrium $[K^+]$ in both groups can significantly increase or decrease, respectively, with a decrease or increase of pH of the pore water (Figure 8). The presence of both K-feldspar and kaolinite in shale, although not in equilibrium, may also control the pore fluid chemistry at a steady state condition with $[K^+]/[H^+]$ (or $[K^+]$ at constant pH) ranging between these two groups depending on the K-feldspar/kaolinite ratio; the higher the K-feldspar/kaolinite ratio, the higher the $[K^+]$. Since the mineralogy of most common shales is rather similar, it is not unexpected that $[K^+]$ can be restricted to a narrow range such as 100 to 300 ppm (big arrow in Figure 8). $[K^+]$ may remain near this level until K-feldspar is significantly consumed. The consumption of K-feldspar may eventually result in the decrease of $[K^+]$ to a level controlled by the illite/kaolinite or illite/smectite equilibrium. The similar $[K^+]$ observed in subsurface brines in sandstones may result from the same mineral control. In some organic-rich shales, pH of the pore fluids may significantly deviate from neutrality due to release of organic acids from kerogen in shales (Carothers and Kharaka, 1978). The decrease of fluid pH tends to increase the equilibrium $[K^+]$ as well as the rate of K-feldspar dissolution; thus, the smectite-to-illite conversion can significantly increase although the shale mineralogy (e.g., K-feldspar/kaolinite ratio) is similar. However, since the K-feldspar dissolution does not limit the rate of smectite-to-illite conversion (Altaner, 1986), the effect of pH on $[K^+]$ in shale fluids is mainly controlled by equilibrium (Figure 8).

Comparison with field data

The experimentally determined kinetic equation can be used to simulate smectite diagenesis under a variety of geological conditions. Since the model suggests that the extent of smectite-to-illite conversion depends on heating rate, $[K^+]$ in the pore fluids as well as initial smectite/illite ratio, we are able to predict the fraction (or percentage) of illite in an I/S sample at a given geological time if we know these parameters. The heating rate of a sample, in turn, depends on the thermal history (geothermal gradient and burial rate) of the host rock formation. The thermal history required to model the smectite-to-illite conversion can also be estimated from the results of basin thermal modeling (Issler and Beaumont, 1989).

The kinetic equation has been tested using data from a large variety of geologic settings worldwide (e.g., the Gulf of Mexico; Vienna Basin; East Taiwan Basin; Salton Trough Geothermal Area; Husana Basin, California). The results show the equation to predict reasonably the extent of the reaction within our knowledge of the variables involved, such as burial history, potassium concentration, thermal gradients, and surface temperature).

Gulf of Mexico. Figure 9 compares the modeling result with field observations for a Gulf Coast shale (Hower *et al.* 1976). The kinetic model can predict the smectite-to-illite conversion by reasonably estimating the geo-

https://doi.org/10.1346/CCMN.1993.0410205 Published online by Cambridge University Press

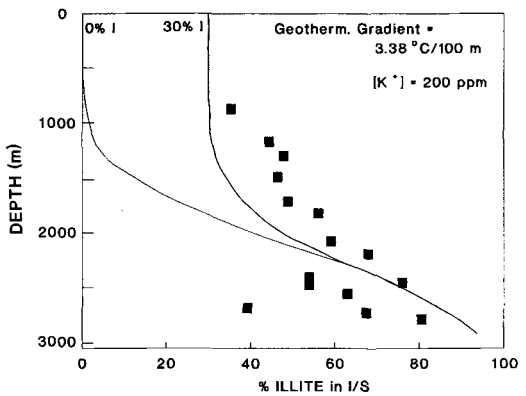

Figure 10. Comparison of modeled (solid lines) and observed (squares) smectite-to-illite conversion for Vienna Basin, Austria (Horton *et al.*, 1985). Two initial I/S compositions, 0% and 30% I in I/S, are assumed in the modeling. Burial rates used are discussed in the text.

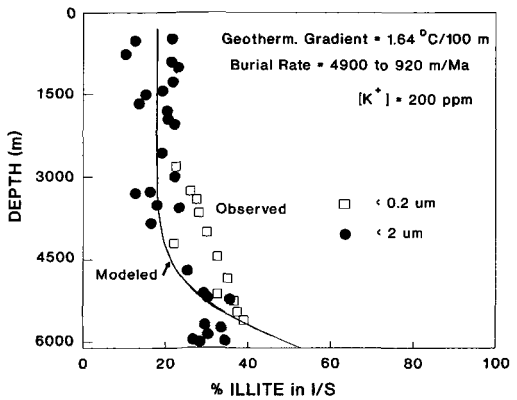

Figure 11. Comparison of modeled and observed smectite-to-illite conversion for East Taiwan Basin (Dorsey *et al.*, 1988). Four combinations of geothermal gradient and [K^+] which give the similar extent of smectite-to-illite conversion as that observed in the field are: 1.64°C/100 m, 200 ppm [K^+]; 1.97°C/100 m, 40 ppm [K^+]; 2.3°C/100 m, 10 ppm [K^+]; 2.62°C/100 m, 2 ppm [K^+].

logical parameters from published information. The Gulf Coast sediments are described as Middle Miocene-Upper Oligocene. A geothermal gradient of 2.62°C/100 meter (m) is used. This is the average of the present day thermal gradients that vary from 2.3° to 2.95°C/100 m (Bodner and Sharp, 1988), assuming a surface temperature of 10°C. The burial rate for the sediment is chosen to give a 40 million year age (Ma) at 5800 m (305 m/Ma to 1520 m depth and then 122 m/Ma). These rates are similar to those reported for the Gulf Coast by McBride *et al.* (1987). Potassium concentration is fixed at 200 ppm as previously discussed. Mineralogical data suggest that K-feldspar is the source of K. This source keeps [K^+] in this shale nearly constant during the smectite-to-illite conversion. When K-feldspar in the shales is completely consumed at depths of around 3660 m (Hower *et al.*, 1976), the [K^+] abruptly drops to a level where both illite and smectite (on the univariant boundary) are stable phases and the smectite-to-illite conversion ceases (Haang, 1990). We model this situation by setting the potassium concentration to zero (which stops further reaction).

Vienna Basin, Austria. Our kinetic model has also been tested against data (Horton *et al.*, 1985) from the Vienna Basin where the burial and thermal history have been well constrained using organic maturation indicators (Johns and Hoefs, 1985; Ladwein, 1988). The smectite-to-illite conversion was modeled for four beds: 17.5 Ma, 16 Ma, 13 Ma, and 12 Ma. The average burial rates for modeling these four beds, respectively, are 162, 119, 82 and 67 m/Ma from the time of deposition of each bed to 8 Ma B. P.; then all four beds were buried at 8 m/Ma from 8 Ma B. P. to present (Johns and Hoefs, 1985; A. Young, personal communication, 1990). The temperature gradients used for modeling these four beds are, respectively, 3.87°, 3.61°, 3.44°, and 3.38°C/100 m, which are similar to the present-day temperature gradient of 3.48°C/100 m (Johns and Hoefs, 1985). [K^+] used is 200 ppm for all beds. Since no information is provided about initial smectite composition, we have plotted two curves by assuming 0% and 30% I in the initial I/S. The predicted depth of significant conversion is in good agreement with mineralogical data (Figure 10). A thermal history similar to that used in this study also predicts organic maturation consistent with the vitrinite field data from the same well (Aderklaa 78 hole, Johns and Hoefs, 1985; A. Young, personal communication, 1990).

East Taiwan Basin. Figure 11 shows the application of the kinetic model to the East Taiwan Basin. Unlike the previous examples, this basin shows little smectite-to-illite conversion even though the sediments are buried to 5490 m. The burial rate (initially at 4880 m/Ma to 3350 m, then slowly decreasing to 915 m/Ma at greater depths) used in modeling is consistent with that reported by Dorsey *et al.* (1988) for this basin. By assuming 200 ppm [K^+] and 10°C surface temperature, the present study quantitatively predicts an abnormally low geothermal gradient of 1.64°C/100 m within the sediments of this basin. The abnormally low geothermal gradient is likely since the rapid accumulation of the young, cold sediments (<4 Ma) may delay thermal equilibration. Alternatively, Dorsey *et al.* (1988) proposed that the rapid decay of the heat flow from the underlying volcanic arc may account for the abnormally low thermal gradient. A third possibility is that the low rate of smectite-to-illite conversion may simply reflect a low [K^+] in the fluid of the studied mudstone. This interpretation is consistent with the mineralogical observation that shows only trace amounts of K-feldspar in the mudstone (Dorsey *et al.*, 1988). The model predicts a geothermal gradient (2.62°C/100 m) similar to that of Gulf Coast area if a 2 ppm [K^+] is assumed

https://doi.org/10.1346/CCMN.1993.0410205 Published online by Cambridge University Press

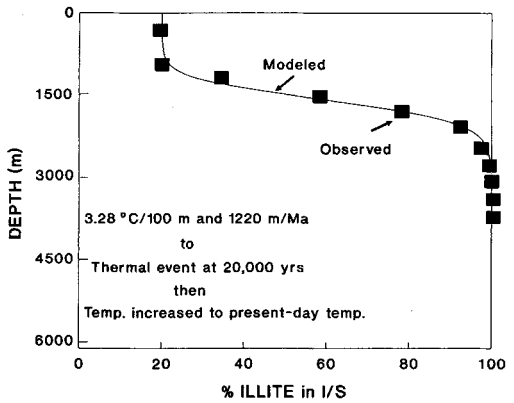

Figure 12. Comparison of modeled and observed smectite-to-illite conversion for Salton Trough Geothermal Area (Jennings and Thompson, 1986). Geological parameters used for modeling smectite-to-illite conversion before the thermal event are geothermal gradient (3.28°C/100 m), burial rate (1220 m/Ma), and surface temperature (20°C). The thermal event that occurs at 20,000 Ma B.P. raises the subsurface temperatures to the present-day profile. See text for discussion.

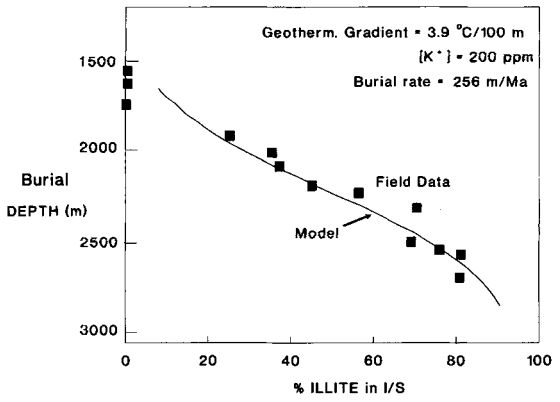

Figure 13. Comparison of modeled and observed smectite-to-illite conversion for Kerckoff well, Huasna Basin, California (Kablanow and Surdam, 1984). The ordinate is burial depth in feet, which includes 1520 m of missing overburden section.

for the pore fluids. Our results suggest that the most likely geothermal gradient of this area during the burial diagenesis ranges from 1.64° to 2.62°C/100 m.

Salton Trough Geothermal Area. Figure 12 shows the opposite extreme to that of the East Taiwan Basin. The field observations of shales from the Salton Trough Geothermal Area show rapid and complete conversion of smectite to illite at a depth of less than 3050 m (Jennings and Thompson, 1986) due to thermal events over the last 20,000 years (Robinson *et al.*, 1976). The rapid conversion can be reasonably modeled using the geological information in this area. The results may place a constraint on the thermal history or $[K^+]$ in the geothermal water during clay diagenesis. The thermal history for this area was modeled in two different steps. Initially, the burial rate (1220 m/Ma) used for modeling was calculated from the estimated age (3 Ma) of the bed at 3660 m (G. R. Thompson, personal communication, 1988). Other estimated parameters used for modeling include the geothermal gradient 3.28°C/100 m, the paleo-surface temperature of 20°C, the initial smectite/illite composition of 20% illite based on near-surface samples, and a $[K^+]$ of 3000 ppm estimated from the present-day subsurface water in the studied area (Salton Trough, S. D. McDowell, personal communication, 1991). The further conversion of smectite to illite during a subsequent thermal event at 20,000 years B.P. was then modeled. It was assumed that during the thermal event the subsurface paleotemperature profile increased linearly to the present-day observed temperature profile. The paleotemperature and smectite/illite composition for each individual bed before the thermal event were used as the initial conditions for modeling smectite-to-illite conversion during the thermal event. Our modeling indicates that, in order to best match the observed I/S field data, a K^+ concentration of 14,000 ppm in the hydrothermal fluid is required. The model suggests that a high $[K^+]$ concentration which is similar to that found in the Salton Sea Geothermal Field (Muffler and Doe, 1968; Truesdell et al., 1981) might be present in the pore fluid during the smectite-to-illite conversion. Alternatively, if the $[K^+]$ concentration is the same during the clay digeneses as observed today (3000 ppm), the model predicts that an abnormally high geothermal gradient (5.9°C/100 m) occurred in this area before the thermal event or that there was a thermal peak present within the thermal event, i.e., the present-day temperature profile is not the maximum.

Huasna Basin, California. In this example, the I/S mineralogical data are used for estimating the thickness of missing overburden section. Figure 13 shows the comparison of field data and the predicted I/S conversion for the Monterey formation in the Huasna Basin, onshore California. The I/S field data are from the Kerckoff well reported in Kablanow and Surdam (1984). The geothermal gradient (3.9°C/100 m), burial rate (256 m/Ma), surface temperature (20°C) and $[K^+]$ (200 ppm) are assumed constant throughout the burial history. The temperature gradient is established by using corrected bottom hole temperature whereas the burial rate is estimated from stratigraphy (Kablanow and Surdam, 1984). The modeling reveals that 1465 m of overburden was eroded from this area. The predicted thickness of the missing section is consistent with that estimated from the stratigraphic data (Kablanow and Surdam, 1984).

Sensitivity studies

Figures 14 to 17 show how the model responds to variations in each geological parameter within a range common during shale diagenesis. With constant geothermal gradient and $[K^+]$, the depth of major con-

https://doi.org/10.1346/CCMN.1993.0410205 Published online by Cambridge University Press

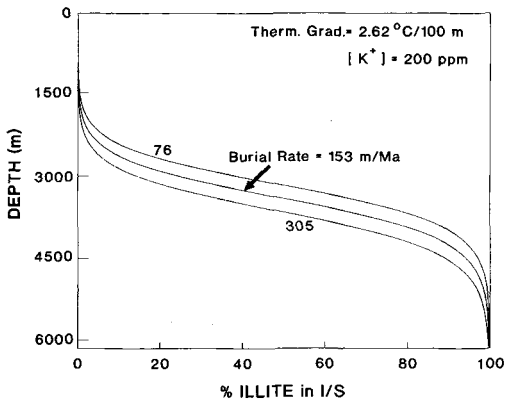

Figure 14. Sensitivity study showing the effect of burial rate on the modeling of smectite-to-illite conversion.

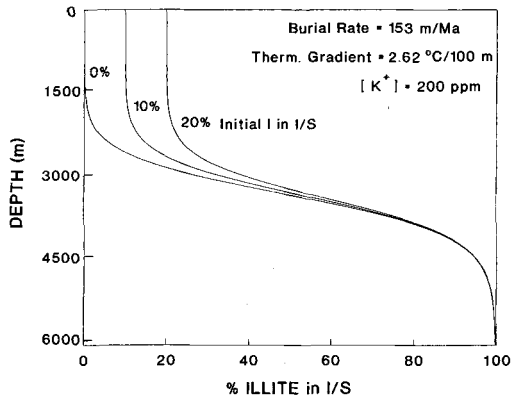

Figure 16. Sensitivity study showing the effect of initial smectite/illite composition on the modeling of smectite-to-illite conversion.

version varies only within a range of 500 m as the burial rate changes from 76 to 305 m/Ma (Figure 14).

On the other hand, a slight change in the geothermal gradient can drastically affect the depth at which the major conversion occurs (Figure 15). The depth can be decreased as much as 1520 m just by changing the geothermal gradient from 1.97° to 3.28°C/100 m. This confirms that temperature is by far the most important factor influencing the smectite-to-illite conversion rate and that the model can be used as a geothermometer to constrain a basin's thermal history.

Figure 16 shows the effect of initial illite percentage in the mixed-layer smectite/illite on the extent of smectite-to-illite conversion. The results show that the effect is initially significant but negligible where there is major conversion.

The modeling results show that the depth of major conversion varies within a range of 400 m as the $[K^+]$ is increased from 100 to 300 ppm (Figure 17). The effect of $[K^+]$ is generally less than that of temperature during shale diagenesis. However, at very low $[K^+]$, a variation from 1 to 10 ppm has an effect as great as from 100 to 1000 ppm.

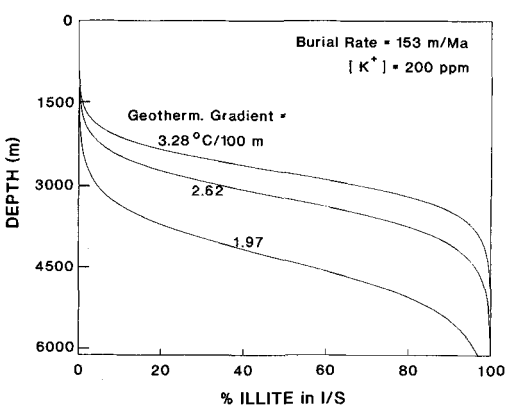

Figure 15. Sensitivity study showing the effect of geothermal gradient on the modeling of smectite-to-illite conversion.

IMPLICATIONS FOR PETROLEUM EXPLORATION

The experimentally derived kinetic model can be used to predict the extent, depth, and timing of smectite-to-illite conversion in a shale if the geological variables such as thermal history are known. Predicting depth or timing of smectite-to-illite conversion, in turn, might be used to risk the sealing integrity of shale, the reservoir quality of an adjacent sandstone, as well as the potential for overpressure (see review in Eslinger and Pevear, 1988). This technique is particularly useful in frontier areas where few well data are available. The burial and thermal history of the target formation required for the modeling can be estimated using a basin modeling program such as reported by Issler and Beaumont (1989).

On the other hand, the model can also be used to constrain basin thermal history if field data for the smectite-to-illite ratio in mixed-layer smectite/illite are available from cores or cuttings. The reaction kinetics provide an independent calibration for other matura-

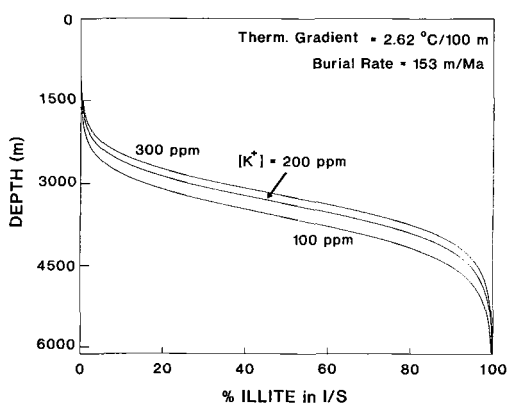

Figure 17. Sensitivity study showing the effect of potassium concentration on the modeling of smectite-to-illite conversion.

https://doi.org/10.1346/CCMN.1993.0410205 Published online by Cambridge University Press

tion indicators such as vitrinite reflectance, TAI or T_{max}. The calibration can be used to refine the proposed thermal history model for a better prediction of hydrocarbon maturation.

In addition, the incorporation of K into the diagenetic illite allows the mean age of illite formation to be dated using standard K/Ar methods. Because K^+ is incorporated into mixed-layer smectite/illite at a rate proportional to the conversion rate, the K/Ar age of the mixed-layer smectite/illite can be calculated using burial history and smectite/illite ratio. The calculated age, when compared with the measured K/Ar age (e.g., Aronson and Hower, 1976) can be used as an independent calibration of the burial history used in modeling smectite/illite conversion (Elliott *et al.,* 1991; Pevear, 1992).

CONCLUSIONS

The kinetics of smectite-to-illite conversion are experimentally quantified. The results show that the conversion rate can be described by a simple rate law that is second-order with respect to the fraction of smectite in the mixed-layer illite/smectite and first-order with respect to K^+ concentration. Our study concludes that temperature, time, and potassium concentration are by far the most important parameters controlling smectite-to-illite conversion.

Our model demonstrates that the variation of $[K^+]$ in shales can be limited to a narrow range (100–200 ppm). Assuming a range of K^+ concentration similar to those found in oil field brines (100–200 ppm), our model can accurately predict the extent of the smectite-to-illite conversion for a number of studied shales (Pytte and Reynolds, 1989) from various depths and ages. This finding has significantly reduced the uncertainty of the model due to the lack of information about $[K^+]$ in the pore fluids of shales and thus improved the applicability of the model to predict smectite-to-illite conversion during shale diagenesis.

The model has also been tested on data from a wide variety of geological settings (Gulf of Mexico, East Taiwan Basin, Salton Trough Geothermal Area). The results show that the equation can reasonably predict the extent of the smectite-to-illite conversion within our knowledge of variables involved.

This quantitative model is useful for modeling the depth and timing of the conversion during shale diagenesis under a variety of thermal histories. The model can be used as a geothermometer to constrain basin thermal history if well data (percent illite in I/S) are available. It can also improve our ability to predict reservoir quality and seal integrity adjacent to a smectite-bearing formation. In addition, the comparison of calculated and measured K/Ar ages of mixed-layer smectite/illite provides an independent constraint on the burial history of a studied formation (Pevear, 1992).

ACKNOWLEDGMENTS

The authors wish to thank our colleagues G. A. Otten for carrying out hydrothermal experiments, T. M. Fleissner for preparing X-ray patterns shown in Figure 5, R. E. Klimentidis for performing TEM studies of starting smectite and experimental run products, Al Young and W. James for testing the kinetic model in a basin modeling program, and E. J. Novotny for critical review and discussion of an early version of this paper. Critical reviews and comments from S. P. Altaner, D. D. Eberl, and E. Eslinger significantly contributed to the improvement of the final version of the paper.

REFERENCES

Altaner, S. P. (1986) Comparison of rates of smectite illitization with rates of K-feldspar dissolution: *Clays & Clay Minerals* **34,** 608–611.

Altaner, S. P. (1989) Calculation of K diffusional rates in bentonite beds: *Geochim. Cosmochim. Acta* **53,** 923–931.

Aronson, J. L. and Hower, J. (1976) Mechanism of burial metamorphism of argillaceous sediment: 2. Radiogenic argon evidence: *Geol. Soc. Amer. Bull.* **87,** 738–744.

Bethke, C. M. and Altaner, S. P. (1986) Layer-by-layer mechanism of smectite illitization and application to new rate law: *Clays & Clay Minerals* **34,** 146–154.

Bethke, C. M., Vergo, N., and Altaner, S. P. (1986) Pathways of smectite illitization: *Clays & Clay Minerals* **34,** 125–135.

Bodner, D. P. and Sharp, J. M., Jr. (1988) Temperature variations in south Texas subsurface: *Amer. Assoc. Petrol. Geologist Bull.* **82,** 21–32.

Boles, J. R. and Franks, S. G. (1979) Clay diagenesis in Wilcox Sandstones of Southwest Texas: Implications of Smectite Diagenesis on Sandstone Cementation: *J. Sed. Petrol.* **49,** 55–70.

Broecker, W. S. and Oversby, V. M. (1971) *Chemical Equilibrium in the Earth:* McGraw-Hill Book Company, New York.

Bruce, C. H. (1984) Smectite dehydration—Its relation to structural development and hydrocarbon accumulation in Northern Gulf of Mexico Basin: *Amer. Assoc. Petrol. Geologists Bull.* **68,** 673–683.

Carothers, W. W. and Kharaka, Y. K. (1978) Aliphatic acid anions in oilfield waters—Implications for origin of natural gas: *Am. Assoc. Petroleum Geologists Bull.* **62,** 2441–2453.

Dorsey, R. J., Buchovecky, E. J., and Lundberg, N. (1988) Clay mineralogy and Pliocene-Pleistocene mudstone, eastern Taiwan: Combined effects of burial diagenesis and provenance unroofing: *Geology* **16,** 944–947.

Eberl, D. D. (1977) The hydrothermal transformation of sodium and potassium smectite into mixed-layer clay: *Clays & Clay Minerals* **25,** 215–227.

Eberl, D. D. (1978) The reaction of montmorillonite to mixed-layer clay: The effect of interlayer alkali and alkaline earth cations: *Geochim. Cosmochim. Acta* **42,** 1–7.

Eberl, D. D. and Hower, J. (1976) Kinetics of illite formation: *Geol. Soc. Amer. Bull.* **87,** 1326–1330.

Eberl, D. D., Srodon, J., Kralik, M., Yaylor, B. E., and Peterman, Z. E. (1990) Ostwald ripening of clays and metamorphic minerals: *Science* **248,** 474–477.

Elliott, W. C., Aronson, J. L., Matisoff, G., and Gautier, D. L. (1991) Kinetics of the smectite to illite transformation in the Denver Basin: Clay mineral, K-Ar Data, and mathematical model results: *Amer. Assoc. Petrol. Geologists Bull.* **75,** 436–462.

Eslinger, E. V. and Pevear, D. R. (1988) *Clay Minerals for Petroleum Geologists and Engineers:* Soc. Econ. Paleontologists Mineralogists Short Course No. 22.

Garrels, R. M. (1984) Montmorillonite/illite stability diagrams: *Clays & Clay Minerals* **3,** 161–166.

Güven, N., and Huang, W. L. (1991) Effect of octahedral Mg^{2+} and Fe^{3+} substitutions on hydrothermal illitization reactions: *Clays & Clay Minerals* **39,** 387–399.

Horton, R. B., Johns, W. D., and Kurzweil, H. (1985) Illite diagenesis in the Vienna Basin, Austria: *TMPM Tschermaks Min. Petr. Mitt.* **34,** 239–260.

Hower, J., Eslinger, E. V., Hower, M. E., and Perry, E. A. (1976) Mechanism of burial metamorphism of argillaceous sediments: 1. Mineralogical and chemical evidence: *Geol. Soc. Amer. Bull.* **87,** 725–737.

Howard, J. J. and Roy, D. M. (1985) Development of layer charge and kinetics of experimental smectite alteration: *Clays & Clay Minerals* **33,** 81–88.

Huang, W. L. and Otten, G. A. (1987) Smectite illitization: effect of smectite composition: in *Program and Abstracts, 24th Annual Meeting, The Clay Minerals Society, Socorro, New Mexico,* 75.

Huang, W. L. (1989) Control on ordering of mixed-layer smectite/illite: An experimental study: in *Program and Abstracts, 26th Annual Meeting, The Clay Minerals Society, Sacramento, California,* 94.

Huang, W. L. (1990) Experimental illitization of smectite and recrystallization of illite: in *Programme and Abstracts, Research Conference on Phyllosilicates as Indicators of Very Low Grade Metamorphism and Diagenesis,* IGCP, Manchester, 10.

Huang, W. L. (1992) Illitic clay formation during experimental diagenesis of arkoses: in *Origin, Diagenesis, and Petrophysics of Clay Minerals in Sandstones,* D. W. Houseknecht and E. D. Pittman, eds., *Soc. Econ. Paleont. Minerl. Special Publication* **47,** 49–63.

Inoue, A. and Utada, M. (1978) Further Investigations of a conversion series of diochahedral mica/smectites in the Shinzan hydrothermal alteration area, northeast Japan: *Clays & Clay Minerals* **31,** 400–412.

Inoue, A., Kohyama, N., Kitagawa, R., and Watanabe, T. (1987) Chemical and morphological evidence for the conversion of smectite to illite: *Clays & Clay Minerals* **35,** 111–120.

Issler, D. R. and Beaumont, C. (1989) Finite element model of the subsidence and thermal evolution of extensional basins: Application to the Labrador Continental Margin: in *Thermal History of Sedimentary Basins,* N. D. Naeser and T. H. McCulloh, eds., Springer-Verlag, New York, 239–267.

Jennings, S. and Thompson, G. R. (1986) Diagenesis of Plio-Pleistocene sediments of the Colorado River Delta, Southern California: *J. Sed. Petrol.* **56,** 89–98.

Johns, W. D. and Hoefs, J. (1985) Maturation of organic matter in Neogene sediments from the Aderklaa oilfield, Vienna Basin, Austria: *TMPM Tschemaks Min. Petr. Mitt.* **34,** 143–158.

Kablanow II, R. I. and Surdam, R. C. (1984) Diagenesis and hydrocarbon generation in the Monterey Formation, Huasna Basin, California: *SEPM Guidebook* **2,** 53–68.

Kacandes, G. H., Barnes, H. L., and Kump, L. R. (1991) The smectite to illite reaction: fluid & solids evolution under flow-through conditions: in *Program and Abstracts, 28th Annual Meeting, The Clay Minerals Society, Houston, Texas,* 95.

Kharaka, Y. K. and Mariner, R. H. (1989) Chemical geothermometers and their application to formation waters from sedimentary basins: in *Thermal History of Sedimentary Basins,* N. D. Naeser and T. H. McCulloh, eds., Springer-Verlag, New York, 99–117.

Ladwein, H. W. (1988) Organic geochemistry of Vienna Basin: Model for hydrocarbon generation in overthrust belts: *Am. Assoc. Petrol. Geologist Bull.* **72,** 586–599.

Lasaga, A. C. (1981) Rate laws of chemical reactions: in *Kinetics of Geochemical Processes: Review of Mineralogy,* A. C. Lasaga and R. J. Kirkpatrick, eds., Mineral. Soc. Amer. **8,** 1–68.

McBride, E. F., Land, L. S., and Mack, L. E. (1987) Diagenesis of eolian and fluvial feldspathic sandstones, Norphlet Formation (Upper Jurassic), Rankin County, Mississippi, and Mobile County, Alabama: *Amer. Assoc. Petrol. Geologist Bull.* **71,** 1019–1034.

Muffler, L. J. P. and Doe, B. R. (1968) Composition and mean age of detritus of the Colorado River delta in the Salton Trough, southeastern California: *J. Sed. Petrol.* **38,** 384–399.

Nadeau, P. H., Wilson, M. J., McHards, W. J., and Tait, J. M. (1984) Interparticle diffractions: A new concept for interstratified clays: *Clay Miner.* **19,** 757–769.

Pevear, D. R. (1992) Illite age analysis, a new tool for basin thermal history analysis: in *Proceeding 7th International Symposium on Water-Rock Interaction*: Y. Kharaka, ed., A. B. Balkema, Rotterdam and Boston, 1251–1254.

Pytte, A. M. and Reynolds, R. C. (1989) The thermal transformation of smectite to illite: in *Thermal History of Sedimentary Basins,* N. D. Naeser and T. H. McCulloh, eds., Springer-Verlag, New York, 133–140.

Reesman, A. L. (1978) Extrapolation of aqueous dissolution data to determine comparative free energies of formation ($C\,\Delta G_f^\circ$) and relative mineral stabilities: *Clays & Clay Minerals* **26,** 217–226.

Reynolds Jr., R. C. (1981) Mixed-layered illite-smectite in a contact metamorphic environment: in *Program and Abstracts, 28th Annual Meeting, The Clay Minerals Society, Urbana, Illinois,* 5.

Reynolds Jr., R. C. (1980) Interstratified layer minerals: in *Crystal Structures of Clay Minerals and their X-ray Identification,* G. W. Brindley and G. Brown, eds., Mineralogical Society London, 249–303.

Reynolds Jr., R. C. and Hower, J. (1970) The nature of interlayering in mixed-layer illite-montmorillonites: *Clays & Clay Minerals* **18,** 25–26.

Roberson, H. E. and Lahann, R. W. (1981) Smectite to illite conversion rates: Effect of solution chemistry: *Clays & Clay Minerals* **29,** 129–135.

Robinson, P. T., Elders, W. A., and Muffler, L. P. J. (1976) Quaternary volcanism in the Salton Sea Geothermal Field, Imperial Valley, California: *Geol. Soc. Amer. Bull.* **87,** 347–360.

Sass, B. M., Rosenberg, P. E., and Kittrick, J. A. (1987) The stability of illite/smectite during diagenesis: An experimental study: *Geochim. Cosmochim. Acta* **51,** 2103–2115.

Środoń, J. and Eberl, D. D. (1984) Illite: in *Mica: Review of Mineralogy,* S. W. Bailey, ed., Mineral. Soc. Amer. **13,** 495–539.

Truesdell, A. H., Thompson, J. M., Coplen, T. B., Nehring, N. L., and Janik, C. J. (1981) The origin of the Cerro Prieto Geothermal Brine: *Geothermics* **10,** 225–238.

Van Olphen, H. and Fripiat, J. J. (1979) *Data Handbook for Clay Materials and other Non-metallic Minerals:* Pergamon Press, New York, 345 pp.

Velde, B., and Vasseur, G. (1992) Estimation of the diagenetic smectite illite transformation in time-temperature space; *Amer. Mineral.* **77,** 967–976.

Whitney, G. and Northrop, H. R. (1988) Experimental investigation of the smectite to illite reaction: Dual reaction mechanisms and oxygen-isotope systematics: *Amer. Mineral.* **73,** 77–90.

Yau, Y., Peacor, D. R., and McDowell, S. D. (1987) Smectite to illite reactions in Salton Sea shales: A transmission and

analytical electron microscopic study: *J. Sed. Petrol.* **57,** 335–342.

(Received 18 February 1993; accepted 3 March 1993; Ms. 2332)

APPENDIX A
KINETIC MODEL DEVELOPED FROM EXPERIMENTAL DATA

Model development

The general kinetic equation for smectite-to-illite conversion at constant temperature and pressure can be written as

$$-dS/dt = k\cdot[K^+]^a\cdot S^b \qquad (A\text{-}1)$$

where S is the mole fraction of smectite in the mixed-layer illite/smectite, t is time, $[K^+]$ is the concentration of potassium ions, k is the rate constant, a and b are constants (Pytte and Reynolds, 1989).

At constant $[K^+]$, the equation can be rewritten as

$$-dS/dt = k'\cdot S^b \qquad (A\text{-}2)$$

where $k' = k\cdot[K^+]^a$. The equation indicates that the decrease of the smectite fraction in the mixed-layer smectite/illite with time is proportional to the b power of the mole fraction of smectite. If b = 2, i.e., the kinetics are second-order with respect to the mole fraction of smectite, the equation becomes:

$$-dS/dt = k'\cdot S^2$$

or (A-3)

$$-dS/S^2 = k'dt$$

Integrating this equation we have

$$1/S = k'\cdot t + I \qquad (A\text{-}4a)$$

where I is an integration constant. With boundary conditions, S = 1 at t = 0, we have I = 1. Eq. 6 becomes

$$1/S = k'\cdot t + 1 \qquad (A\text{-}4b)$$

This suggests that if our experimental data fit this equation then plotting 1/S *vs* t will give a straight line. The mole fractions of smectite (S) at different times, which we experimentally measured at near-constant $[K^+]$, were used to calculate k′ using linear regression. The results are plotted in Figure 4. Our data are reasonably consistent with linear relationships (the scattering of data is mainly attributed to the variation of starting smectites from one batch to another). This suggests that smectite-to-illite conversion can be described by second-order kinetics with respect to smectite fraction (S^2 in Eq. A-3).

Since $k' = k\cdot[K^+]^a$, and therefore $\log k' = \log k + a\cdot\log[K^+]$, we are able to obtain the "a" value from the slope of log k′ *vs* $\log[K^+]$ at constant temperature (Figure 5). Our results at 300°C, the temperature studied in the most detail, show that "a" equals 1.07. By assuming the same "a" value (=1), our data at the other three temperatures reasonably fit straight lines within the experimental uncertainty (this was done using linear regression with constant slope). This suggests that the kinetics of smectite-to-illite conversion are first-order with respect to K concentration (i.e., $k' = k[K^+]$). Thus, the overall equation for smectite-to-illite conversion becomes:

$$-dS/dt = k\cdot[K^+]\cdot S^2 \qquad (A\text{-}5)$$

The effect of temperature on the conversion can be calculated from our experimental data with the procedure described below. The average log k′ value for a wide range of $[K^+]$ at each temperature was determined from the lines at $\log[K^+] = 0$ in Figure 5. (Note that at $\log[K^+] = 0$, the k values are equal to the corresponding k′ values because $k' = k\,[K^+]$). These are −0.25, −0.91, −1.13 and −1.80 respectively at 325°, 300°, 275°, and 250°C. The average activation energy (Ea) and frequency factor (A) for all $[K^+]$ can thus be calculated by plotting log k vs 1/T (Figure 6) using the Arrhenius equation:

$$k = A\cdot\exp(-Ea/RT) \qquad (A\text{-}6a)$$

or

$$\ln k = -(Ea/R)(1/T) + \ln A \qquad (A\text{-}6b)$$

The slope and intercept of the Arrhenius plot give, respectively, Ea = 28 Kcal/mole and $A = 8.08 \times 10^4$ sec^{-1} $mole^{-1}$ liter.